CHAPTER 21

PRINCIPLES OF MAGNETIC RECORDING

Magnetic recording is based on remanence, i.e. on the possibility of writing stable or metastable magnetization configurations within a material. The information carrying medium is the heart of any recording (or storage) system. Of course it is complemented by write, erase, and readout devices.

The first part of this chapter describes the basic principles, and gives a short overview of the magnetic recording processes actually used today. They all rely on thin films for accessibility reasons.

The second part deals with the information supporting media. They can be particulate, or granular, media, in which information is written in the form of magnetised regions much larger than the grains, and not to be mixed up with domains. The medium can also be homogeneous, free of defects, and devoid of coercivity. In the latter case, domains in their equilibrium configurations are well suited to the storage of digital information, with the advantage that this information can be moved around within the medium. In this case the medium remains fixed (bubble memories), while the information on band or disk systems can be accessed only by moving the medium.

The third part is devoted to the writing processes. We describe the magnetic (or inductive) process, in which magnetization is written very locally by an applied field through a write head (which can generally also be used for reading). The thermomagnetic process involves localised heating of the medium through laser impact, with simultaneous application of a magnetic field. It is associated with the magneto-optical memories.

The fourth and last part is devoted to magnetic readout. In the inductive process, information is generally read by the write head. The magnetoresistive process involves a specialised head which cannot be used for writing, but which indirectly leads to a sizeable increase in the maximum storage density.

1. INTRODUCTION

The father of magnetic recording is the Danish engineer W. Poulsen. In 1898, he demonstrated an instrument which he called the *telegraphone,* the ancestor of our modern tape recorders. The telegraphone involved a small electromagnet, the forerunner of our present write and read heads, and the recording medium was just a hard steel wire (piano string).

The crucial progress which led to the industrial development of analogue recording, in its audio form from 1948 and its video form from 1951, involved two steps. One was the invention of the analogue recording process based on *AC-biasing,* by Carlson and Carpenter in 1921, and its rediscovery and improvement by German engineers during World War II. The other one was the development of various types of *magnetic tapes.**

On the other hand, the development of the first computers created, at the beginning of the 1950's, the need to store *digital* information in a manner that would combine capacity and speed of access. The first disk drive, the RAMAC, was produced by IBM in 1957. It already involved the main principles of the present disk units, although its performance may appear quite modest to us today. In particular its maximum information density was 2 $Kbits.in^{-2}$ (300 $bits.cm^{-2}$), and its data transfer rate was 70 $Kbits.s^{-1}$. Its total capacity, 5 Mo, was reached by putting together no less than 50 disks with diameter 24 in (60 cm). In 1999, a typical hard disk unit (a commercial IBM product) features a maximum information density of 5.7 $Gbits.in^{-2}$ (0.88 $Gbits.cm^{-2}$), a data transfer rate of 118 $Mbits.s^{-1}$, and it can store 6.5 Go on two 2.5 in (6.35 cm) diameter disks. The conservative theoretical limit [1] of 40 $Gbits.in^{-2}$ (6.2 $Gbits.cm^{-2}$), the superparamagnetic limit, could already be reached by 2003-2004.

While the well-established technologies (longitudinal magnetic recording on disks and tapes) further progress towards their theoretical limits [1, 2], other principles are investigated in the laboratory, and could emerge in the next few years: perpendicular recording [3], "quantised" or "patterned" disks [4], and magnetic random access memories (MRAM) [5] using the magnetoresistance of a tunnel junction between two ferromagnetic metals [6].

In view of this particularly fast evolution, this chapter aims mainly at describing the principles, and the unchanging physical limitations of magnetic recording processes, while giving fairly little detailed informatoin on the technological aspects. The reader who wants to keep abreast of the state of the art should look up the literature.

---

* Of course we should not forget the development of electronics, triggered by the invention of the triode in 1906.

It must also be mentioned that, within the general area of re-writable mass storage technologies, non-magnetic processes are also being investigated. Some of them were already convincingly tested, e.g. holographic [7] or microprobe storage [8].

It is natural to end this introduction by drawing the reader's attention on some recent books dealing with the most basic aspects of magnetic recording [9-13].

2. OVERVIEW OF THE VARIOUS MAGNETIC RECORDING PROCESSES

The most common recording process is so-called longitudinal recording. Its principle is shown in figure 21.1. The recording *medium* is a thin magnetic layer, with thickness h, which we will discuss later. It is supported either by a flexible plastic substrate (tape and floppy disks), or by a rigid substrate, usually made of aluminium (hard disk). The write head consists of a magnetic circuit involving a small gap, with thickness g, and an excitation coil with n windings.

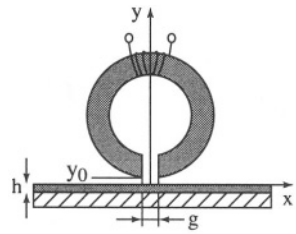

Figure 21.1 - Principle of longitudinal magnetic recording

The magnetic layer is submitted to the stray field, which is localised near the gap. We can thus consider that only a small region of the layer, with length roughly equal to the gap thickness g, and with width W >> g equal to that of the head, is submitted to the so-called write field produced by the head.

As we willl see, the essential component in this configuration is parallel to the axis Ox of the track.

2.1. ANALOG RECORDING

Let the tape run at constant speed v while a current I (t) proportional to the instantaneous value of the signal to be recorded is passed in the excitation coil of the head. Then the track, assumed to be initially demagnetised, will have along its length a magnetization distribution M (x) where x = v t, the space image of the time signal I (t).

We will see further how this space distribution of magnetization can, in turn, be changed into a time signal identical to the initial signal (readout). For the moment, we want to look more precisely at the write process.

Figure 21.2 shows the classical description of the static response of a rather hard ferromagnetic sample to an applied field. In particular, let us assume that the initially demagnetised sample is submitted to a field excursion with amplitude H (a field starting from zero to a maximum value H, and then returning to its initial zero value). There remains a so-called remanent magnetization M_r which is –at least insofar as H remains small enough– a growing function of H, with a striking non-linear character (fig.21.2-b).

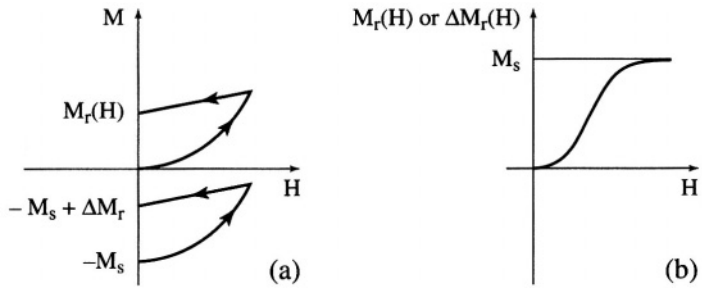

Figure 21.2 - Response of a coercive material to a field excursion

M_r and ΔM_r: remanent magnetization and its variation;
H: amplitude of the field excursion.

A qualitatively identical behavior is observed if we start, for example, from negative saturation, and plot the *variation* in remanent magnetization as a function of the amplitude of a positive field excursion (see lower loop in fig. 21.2-a).

These measurements are usually performed on size scales and under excitation configurations that are very different from those of recording on thin films (see chap. 2 and 26). However, in the latter case, we do not expect very different results, at least qualitatively and provided that:

- the thickness g of the gap and that, h, of the film, remain much larger than the lengths characteristic of the microstructure in the sample;
- the translation of the track at velocity v in the presence of a constant write current can be considered as equivalent to a field excursion with duration g/v, with the medium remaining fixed;
- the demagnetising effect associated in particular with the finite length of the region submitted to the write field is taken into account by correcting the applied field.

Then the response curve of the film, in terms of the remanent magnetization $M_r(I)$ or of the variation in remanent magnetization that are locally induced on a moving track by a write current with instantaneous value I, retains the shape of the $M_r(H)$ curve of figure 21.2-b, with marked non-linear character. Linearity can be improved by working around a point other than origin. Thus, from figure 21.2-a, it is tempting to work around the inflection point.

Actually, things are bit more complicated, but this DC biasing process has actually been used until a much more efficient process, AC biasing [13], was developed. The

latter is based on the use of the *anhysteretic* curve, already introduced in § 2.5.1 of chapter 3 and in § 4.1.3 of chapter 6. We recall that this involves measuring the magnetization M_{an} created by a static field H when an *AC "unpinning" field is simultaneously applied,* with a slowly decreasing amplitude but starting from a value much larger than the coercive field. The anhysteretic magnetization $M_{an}(H)$ is measured when the amplitude of the auxiliary AC field is reduced to zero, but actually the AC field has only a very small influence on the final value of M_{an} as soon as its amplitude is much smaller than the coercive field H_c. The procedure is repeated for each new value of the static field H. The $M_{an}(H)$ curve thus obtained shows no hysteresis, and it remains linear up to a value of M_{an} typically around $0.4\ M_s$ with a slope only limited by demagnetising effects. In other words, the initial *internal* anhysteretic susceptibility is infinite but, except in a toroidal geometry, the demagnetising field effect always leads to a finite *external* anhysteretic susceptibility χ_{an}.

Assume we work at a point of the anhysteretic curve defined by magnetization M_{an} and an applied external field H_0. After the AC unpinning field is suppressed, we now decrease H_0 to zero. Because the material again has coercivity, it is clear that there remains a remanent magnetization practically equal to $M_{an}(H_0) = \chi_{an} H_0$.

The recording head is fed with a *carrier current* with high frequency (typically 70 kHz for audio tapes), and with large amplitude. The write signal which is superimposed on the carrier has a frequency much lower than 70 kHz in audio recording, and it can be considered as static on the scale of the period of the carrier current. Consider a given region of the tape. As it passes across the head, it is submitted to an AC field with an amplitude that first grows to a nominal value H_{acn} much larger than the coercive field, and then tends to zero. Simultaneously, the write field grows to a nominal value H_{en}, then also goes to zero. This decrease is, in both cases, due to the fact that the region of interest moves away from the gap, and we will see later how it can be described.

We thus perform, in the region of interest of the tape, the experiment we described above, leading, at least to a first approximation, to the writing of a local magnetization proportional to the instantaneous write current.

This distribution of magnetization M and $\Delta M_r(x)$ thus written on the tape can later be recovered in the read step, which converts it into an electric signal in time V(t) through the reverse process: the recorded tape is passed at constant velocity v across a so-called read head, built in exactly the same way as a write head. Actually, the same head can be used for reading or writing. The principle involved in reading is induction. The voltage V(t) developed across the coil is proportional to $d\Phi/dt$, where $\Phi(t)$ is the instantaneous flux induced in the magnetic circuit of the head. We will see in § 5 that $\Phi(t)$ is proportional to M (x = vt), so that the signal picked up, V(t), is in fact the image of dM/dx. This leads to an enhancement of the high frequencies, called

harmonic distortion by electronic engineers. This distorsion effect at reading, as well as another one related to recording, are corrected by filters in the amplification chain.

This section devoted to analog recording was brief. This reflects the tendency which will probably be confirmed in the coming years, viz the gradual replacement of all analog recording systems by digital systems, both in the audio (sound recording) and in the video (image recording) area.

The reader can find some complementary information in the recent books by R.M. White [14] and by P. Ciureanu and H. Gavrila [15]. The rest of this chapter only deals with *digital* recording.

2.2. DIGITAL RECORDING

Digital recording is, in its very principle, much simpler than analog recording. In the recording medium (tape or disk), it only aims at producing two values of magnetization, $+M_S$ or $-M_S$, M_S being the remanent magnetization that corresponds to the saturated loop. A track in a recorded digital tape or disk therefore consists in regions of alternating magnetization, with unequal lengths. These of course correspond neither to individual magnetic domains, nor to a *bit,* given the variety of *encoding systems* that are used.

Here we just mention this encoding problem. The interested reader should look up specialised books and papers [12, 14, 16]. A track in a tape or a disk is subdivided into small equal intervals (expressed indifferently in terms of length L or duration $T = L/v$), in which the binary data *(bits)* are arranged in a row.

The contents of the track can then be read in an understandable way only insofar as each of these intervals is recognised and identified through its rank in the sequence. Without going into details, this is obtained by synchronising the readout with the motion of the recorded track.

The simplest code consists in assigning one of the magnetization polarities the value 0 and the other the value 1. We must however remember that, as we willl see in detail later, the signal provided by a read head is not directly the written magnetization, but its *derivative* with respect to the coordinate x measured along the track. This means that only t*ransitions,* i.e. magnetization reversals, are in fact detected. It is thus clear that, if for some reason a transition is not detected in a sequence of binary data, the following bits will all have the wrong value (the value complementary to their real value). This is called error propagation.

A first sophistication possibility for the encoding scheme consists, in order to eliminate this problem, in using directly the transitions themselves. The convention is then that the presence of a transition, whatever its polarity, in a given readout interval corresponds to a binary “1”, while the absence of such a transition corresponds to binary “0”.

Other considerations (error detection, readout synchronization...) lead to further sophistication. Auxiliary transitions that do not correspond to data bits are then added. This implies, for a given information content, more cluttering of the track.

2.3. PERPENDICULAR RECORDING

In longitudinal magnetic recording, the demagnetising field associated with the finite length d of the uniformly magnetised region between two transitions grows with the h/d ratio. This demagnetising field tends to destroy the magnetization in the region of interest, and we understand how this leads to a lower boundary for distance d, hence to a limitation in the storage capacity.

One way around this difficulty is to magnetise the sample in the direction, not parallel to the plane of the film, but perpendicular to it. This is referred to as *perpendicular recording*. In this case, the demagnetising field decreases with the ratio d/h. On the other hand, it is a maximum for d >> h. This is why media with high uniaxial anisotropy, involving easy magnetization directions perpendicular to the film, must then be used.

Purely magnetic perpendicular recording on coercive media has been for years and is still at the laboratory stage. A strong revival of interest in this technique is, however, observed at present [2, 3]. Besides, magneto-optical storage as well as domain propagation memories are based on this "perpendicular" magnetization configuration and they have been commercially available for several years.

2.4. MAGNETO-OPTICAL RECORDING

These memories implement the perpendicular recording mode we just described, but writing and reading are performed optically [17, 18]. One of the main advantages of this technique is that, unlike in purely magnetic systems, the read or write head does not need to fly at a tiny height over the disk surface. The system is thus less sensitive to dust, which allows the disk to be removed and replaced at will.

Apart from a strong uniaxial anisotropy, with easy magnetization direction perpendicular to the plane of the film, the materials used, again in thin film form, must have, for reasons that will become clear soon, a large wall coercivity.

The writing process, called thermomagnetic, is based on a rapid decrease of the coercive field with temperature.

If a write field H smaller than the coercive field is applied to the whole film, along its normal Oz, at room temperature, there is by definition no alteration in the magnetization distribution of the medium. However, if a small region of the film is heated by a laser beam focused down to the diffraction limit, the coercive field can locally become smaller than H. The heated region then saturates in the direction of the

applied field. This leads to the writing of stable bits, with size roughly equal to that of the laser's footprint on the film (hence of the order of the wavelength).

The readout process uses the polar Kerr effect, which is described in detail in chapter 13. The same laser is used for readout and writing, but of course at different output levels (typically 2 mW for readout and 10 mW for writing), at a wavelength λ in the near infrared for the first equipments ($\lambda \approx 0.8\ \mu m$). The tendency is of course to go to shorter wavelengths to decrease the size of a bit.

2.5. DOMAIN PROPAGATION MEMORY

All the processes described above use the fact that the M (H) relation, as determined experimentally on samples with typically centimetre-range size, remains valid for micron-range sizes, possibly with corrections for the demagnetising field effect.

This is made possible in granular and paniculate media, or even in continuous media involving defects, by the existence of characteristic sizes (the size of grains or particles, average distance between particles, size of defects) that always remain much smaller than the size of the regions submitted to the write field.

The situation is radically different if the medium is continuous, i.e. free of microstructure. The *wall coercive field* (the minimum field needed to unpin the wall) is then zero or very weak, and nothing prevents the film from taking on a domain structure strictly governed by magnetostatic equilibrium considerations. It is obvious that an *arbitrary* distribution of magnetization then cannot be imposed on the film, except with tricks. Memories can nevertheless be made with this type of material. They use in a very special way the free propagation property of walls. These devices are known as domain propagation memories, or more comonly *bubble memories.*

We will restrict their description to a brief discussion of their principle, because they did not encounter the expected success. They did however raise beautiful problems in magnetism, and the reader interested in the subject can look up the book by Eschenfelder [19].

Consider a thin film, with thickness h, spontaneous magnetization M_s, uniaxial anisotropy constant K, with easy axis Oz perpendicular to the plane of the film. The most stable equilibrium state in zero field for such a geometry depends on the ratio $K/\mu_0 M_s^2$. Two extreme situations can be predicted.

If $K/\mu_0 M_s^2 << 1$, the demagnetising field energy is dominant, the magnetization is parallel to the plane of the film, and the domain structure depends on the sample shape in the plane.

If $K/\mu_0 M_s^2 >> 1$, the uniaxial anisotropy forces a magnetization direction parallel to Oz, and there appears a stripe domain structure (fig. 21.3-a). Its period d results from a compromise between the magnetostatic energy (which grows with the ratio d/h), and the wall energy (proportional to h/d).

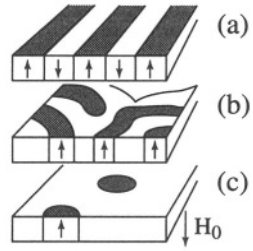

Figure 21.3
Periodic stripe, maze and cylindrical domains (garnets for bubble memories)

Actually, the naturally observed structures are rather of the two-dimensional maze type (fig. 21.3-b), but the band width remains very close to the prediction of a one-dimensional model. If a bias field $\mathbf{H_0}$ parallel to Oz is applied and is large enough, the film of course saturates in the direction of $\mathbf{H_0}$. It can however be shown that, if $\mathbf{H_0}$ is not too large, stable cylindrical domains, with radius r, with magnetization opposite to $\mathbf{H_0}$ (bubbles!) remain, isolated within a region magnetised along $\mathbf{H_0}$.

These domains are stable if H_0 remains between two limits, H_b and $H_c > H_b$.

H_c is called the *collapse field.* When H_0 becomes larger than H_c, the bubble, which had finite radius r equal to r_c, collapses and disappears abruptly. If H becomes smaller than H_b, the cylindrical domain becomes unstable with respect to elliptic deformation: the bubbles change into stripes.

In the interval $\{H_b, H_c\}$, the bubble radius r is a decreasing function of H, continuous up to $r = r_c$. The bubble shape is stable with respect to small perturbations, and the bubbles can move very freely within the film, under the influence of small gradients in the bias field.

This property is used in so-called shift registers: the bubbles are shifted, in synchronism with a clock, along a track made of soft alloy (Permalloy) patterns deposited on the surface of the material.

These patterns are submitted to a propagation field which is rotated parallel to the film. The field gradients they create have the dual role of guiding the bubbles and shoving them along the track. The presence of a bubble in a sequence very naturally corresponds to a binary "1", whereas its absence correspond to "0".

The register includes a bubble generator/erasor which writes or modifies the data sequence during its circulation, and a detector which reads the information.

The device is equivalent to a more classical moving medium storage system (based on disk or tape), with the advantage of complete absence of mechanical motion, hence in particular of high insensitivity to shock and vibration.

On the other hand, the capacity remains very much smaller than that of disks, and the access times very much larger than those of semiconductor memories.

Bubble memories are only used today in very special applications (space and aeronautics), where their shock and radiation resistance, together with their non-volatility (the information is retained in case of power failure), are essential criteria.

3. RECORDING MEDIA

The various magnetic media used in recording belong to three categories. Particulate media consist of fine magnetic particles, spread in a polymer matrix. Granular media usually are actually ferromagnetic polycrystalline metals or alloys. Finally "continuous" and homogeneous media are thus called to distinguish them from granular media, and they can be either single crystalline, or amorphous.

More basically, one can distinguish between coercive and non-coercive media. The particulate and granular media are then in the first category, while the continuous homogeneous media are normally in the non-coercive range.

All media, as was already mentioned, are available in the form of thin films deposited on a substrate.

3.1. PARTICULATE MEDIA

The films are obtained by spreading on the substrate a polymerisable resin that contains a suspension of a fine powder, generally iron oxide (γ-Fe_2O_3).

The γ-Fe_2O_3 grains are typically shaped like prolate ellipsoids, with major axis $a \sim 1\,\mu m$ and minor axis $b \sim 0.2\,\mu m$.

3.1.1. Stoner-Wohlfarth model

The Stoner and Wohlfarth model is the simplest description of such a composite. It is analysed in detail in chapter 5. It predicts a hysteresis loop characterised by a coercive field of the order of 1/2 H_a where H_a is the total anisotropy field (including the shape effect) of the particle. It is based on two strong assumptions.

One is that, within a particle, magnetization reverses through uniform rotation. The other is that interactions between particles are negligible.

Actually, the coercive field measured in these composites is two to three times lower than the predictions of this model (typically $\mu_0 H_C \sim 0.03$ T instead of 0.09 T), which questions the validity of these assumptions.

Two non-uniform rotation mechanisms are analysed in detail in chapter 5. They do lead to a decrease in coercive field, provided however that the total anisotropy of the particle is mainly magnetostatic in origin (shape anisotropy).

It was established [20] that shape anisotropy contributes typically 2/3 of the total anisotropy in the γ-Fe_2O_3 particles used in recording, while 1/3 is due to magnetocrystalline anisotropy. Measurements performed on a single particle [21] seem to confirm that these non-uniform rotation mechanisms play a dominant role in magnetization reversal.

The effect of dipolar interaction between particles was not treated in chapter 5. This is a complex problem which can only be solved in a general way by numerical simulation.

Here we just discuss a *plausibility* argument showing that interaction decreases the coercive field. Consider a set of elongated particles, with their axes all parallel to a common direction Oz. Initially, all the particles are supposed to be magnetised in the same direction +Oz. A static magnetic field $H_z = -H (H > 0)$ is then applied. Assume that the magnetic moment in each particle is rotated by the same small angle θ: then there appears a restoring torque acting on each of these moments. What is the contribution just from the interaction to this torque?

This purely dipole interaction can be roughly estimated using an approach similar to that used in the theory of dielectrics (Lorentz field). Assume the "cavity" remaining when a given particle, assumed to be point-sized, is taken out of the composite is on average a sphere. The interaction field acting on a given particle is thus approximately the field that acts within a spherical cavity dug in a uniformly magnetised medium. The relevant magnetization here is that corresponding to the deviation θ, viz $c M_s \sin\theta$ (where c is the volume fraction of particles), and the interaction field is $(1/3) c M_s \sin\theta \sim (1/3) c M_s \theta$. Its direction is *perpendicular* to Oz and it is oriented so that the restoring torque, with modulus $(1/3) \mu_0 c M_s^2 \theta$, is *negative.* The restoring torque acting on the moment of a particle is thus:

$$\Gamma = [2K - H M_s - (1/3) \mu_0 c M_s^2] \theta \qquad (21.1)$$

We see that the stiffness $d\Gamma/d\theta$ vanishes, hence that the position $\theta = 0$ becomes unstable, for a value of H smaller than $2K/M_s$. This value is, in the case under study, the coercive field of the isolated particle.

This simple model thus predicts a decrease in H_c proportional to the volume fraction of the particles in the composite, in agreement with experiment.

3.1.2. Superparamagnetism in particulate media

Around its stable state, with magnetization either along Oz ($\uparrow$) or along the opposite direction ($\downarrow$), the energy of the particle is a quadratic function of the direction cosines α and β of magnetization. The mean energy associated, at thermal equilibrium, with each of these degrees of freedom is, from the equipartition theorem of statistical physics, $(1/2) k_B T$, where k_B is Boltzmann's constant. For an isolated particle with volume V, we have: $V(<\alpha^2> + <\beta^2>) (1/2) (N_b - N_a) \mu_0 M_s^2 = k_B T$, whence:

$$<\alpha^2> + <\beta^2> = 2 k_B T / [(N_b - N_a) \mu_0 M_s^2 V] \qquad (21.2)$$

We here assumed that the anisotropy is solely due to the shape effect (see chap. 5). If the volume of the particle decreases, the amplitude of the thermal oscillation in the magnetization direction increases, and it is clear that the probability for spontaneous reversal of magnetization becomes sizeable.

According to Boltzmann statistics, the frequency f of spontaneous reversals is given by:

$$f = f_0 \exp[-(N_b - N_a)\mu_0 M_s^2 V / 2 k_B T] \quad (21.3)$$

where the pre-exponential factor f_0 is the number of attempts per unit time. A good approximation for f_0 is the width of the natural gyromagnetic resonance line of the particle (see chap. 17). As an indication, f_0 is probably of the order of 50 to 500 MHz for a γ-Fe_2O_3 particle. The frequency of spontaneous reversals becomes of the order of f_0 for $(1/2)(N_b - N_a)\mu_0 M_s^2 V = k_B T$, and, if we take $V \sim ab^2$, with b/a = 0.2, we see that this occurs at room temperature for b = 3 nm hence a = 15 nm.

The spontaneous reversal frequency is then large on the scale of any quasi-static experiment. In particular, no remanent magnetization is then measured! This behavior is referred to as superparamagnetism, in analogy with the paramagnetism of atomic moments. This regime must absolutely be avoided in memories [1]. Fortunately, the variation of f with the ratio V/T is exponential, so that, for the γ-Fe_2O_3 classically used ($a \sim 1\ \mu m$ and $b \sim 0.2\ \mu m$), the average time between spontaneous reversals is already much larger than the average lifetime of a generation of memories.

Superparamagnetism is treated in detail in a recent review paper [22], and briefly in chapters 4 (§ 2.3) and 22 (§ 3.1) of the present book.

3.2. GRANULAR MEDIA, METALLIC THIN FILMS

As we will see later, reducing the thickness of the magnetic film makes it possible, in the purely magnetic recording process, to increase the surface density of information, hence the storage capacity. However, the read signal amplitude is roughly proportional to the product of the thickness h by the spontaneous magnetization M_s, hence it is desirable to increase M_s when h is reduced.

The use of metal and alloy films is a considerable progress with respect to Fe_2O_3 based composites, because both the intrinsic value of magnetization and the filling factor are increased.

The metallic materials used in longitudinal magnetic recording are Co based alloys [23]. The films are textured and polycrystalline, with typical grain sizes of the order of 10 nm, and thickness around 20 nm. The local easy magnetization direction is oriented at random within the film plane. The magnetization processes are more complex than in single domain particle composites, because the interactions between grains are strong. The coercivity of these films is observed to be strongly correlated to their microstructure, which usually involves several characteristic scales (grains, subgrains, phase boundaries).

In several respects, however, the behavior of these granular media is not considered as very different from that of a collection of isolated particles. This is for example the current assumption for calculating their superparamagnetic limit [1, 2].

The materials for magneto-optical recording are usually amorphous R-FeCo type alloys (R being a rare earth metal Tb, Gd, Dy), with so-called *sperimagnetic* magnetic structure. The moments of the terbium and iron (and cobalt) atoms then make up partially disordered sublattices, with resulting moments in opposite directions (see fig. 4.21).

This structure, special to amorphous materials, is reminiscent of the ferrimagnetism of crystallised compounds such as ferrites. As in some ferrimagnets, these materials feature a compensation temperature, where the mesoscopic magnetization $\mathbf{M_S}$ goes to zero and changes sign. We note that the apparently physically sensible conclusion that, since the mesoscopic magnetization is zero, there must be no Kerr or Faraday rotation at the compensation temperature is wrong. The rare earth-metal and transition-metal "sublattices" contribute in a nearly additive way to the magneto-optical effect, and they have different contributions even when the absolute values of their magnetic moments are equal. The information can therefore be read at the compensation point too.

Finally, these materials feature, at least under some preparation conditions, both a strong perpendicular anisotropy and coercivity that is high at room temperature, and rapidly decreases with temperature. The anisotropy observed ($\mu_0 H_a$ is typically of the order of 1 to 2 T) is usually explained by a pair orientation order induced during the film deposition, and favored by the symmetry of this special forming process.

The origin of coercivity in these amorphous materials, assumed to be free of microstructure, is a question which deserves some more thought and comments.

A single domain sample of a *perfect* uniaxial material, with anisotropy field $\mathbf{H_a}$ larger than its demagnetising field $\mathbf{NM_s}$, is *metastable* in the saturated state. Its magnetization reverses under a uniform inverse magnetic field only when the uniform rotation mode becomes unstable, which, in thin film geometry, requires an external field at least equal to $\mathbf{H_a - M_s}$. In such a material, the coercive field is thus, to a first approximation, equal to $\mathbf{H_a - M_s}$. This behavior is indeed observed in single-crystal or amorphous films used in bubble memories (see § 2.5). However, this is a very narrow view of coercivity. Consider now, not the saturated single domain state, but a multi-domain state, for example the stablest state in zero field (we saw in § 2.5 that this is a stripe domain structure, with zero mean magnetization). The curve of magnetization vs external field obtained starting from this state –which can be called an initial magnetization curve– features, as in soft materials, an initial part that is linear, and at any rate does not have an appreciable threshold effect. This means zero coercivity. Of course this results from the fact that the magnetization process operating in this case is wall displacement. In a perfect material, nothing opposes this displacement, and wall coercivity is zero.

In usual uniaxial materials, there are various kinds of defects, in other words a microstructure, more or less pronounced. As a consequence, the reversal field for the saturated film is smaller than the theoretical value $\mathbf{H_a - M_s}$ because the presence of defects leads to weak points on which reversal starts before the uniform rotation mode

becomes unstable. This process may be thermally activated, in which case the weak points are rather called nucleation sites.

The defects also have the opposite effect, as they are pinning points for the walls. This leads to non-zero wall coercivity, which can in particular stabilise states which would be unstable from the magnetostatic point of view (see § 2.5).

The result of these two effects is that the magnetization curve or the hysteresis loop now have a local meaning. In particular, the size of the analysed region has no influence insofar as it remains much larger than the length characteristic of the microstructure and than the film thickness.

In the R-FeCo alloys used in magneto-optical recording, the presence of spatial anisotropy fluctuations on a mesoscopic scale (whether the modulus of the anisotropy field or the orientation of the easy axis is involved) and the existence of a compensation point are considered as the essential ingredients to explain coercivity and its thermal variation [18]. The fluctuations lead directly to *coercive energy or pressure* terms independent of magnetization M_s. As a result, the coercive field H_C is inversely proportional to M_s, hence it diverges at the compensation point.

3.3. CONTINUOUS MEDIA: EPITACTIC SINGLE CRYSTAL FILMS AND HOMOGENEOUS AMORPHOUS FILMS

In domain propagation memories, the information supporting media must be free of microstructure and even of localised defects. Two types of materials satisfy this demand: the single crystal films obtained on a single crystal substrate, and homogeneous amorphous films.

In fact, while both types of materials have been developed in the laboratory, only epitactic films of magnetic garnets on a non-magnetic garnet have been used in commercial devices.

The magnetic garnets have the basic formula $R_3Fe_5O_{12}$, where R is a rare earth atom or yttrium. Innumerable substitutions are possible, both on the iron sites and on the rare earth sites, and the compositions used for bubble memories involve as many as ten components.

The non-magnetic substrate that is classically used is gadolinium gallium garnet $Gd_3Ga_5O_{12}$, commonly designated by the acronym GGG. The reader will find a lot of information on bubble memory materials in reference [19].

4. THE WRITE PROCESS

There are two main processes for creating or altering the magnetization of a small region in a magnetic thin film: the local application of a field using a write head, and thermomagnetic writing using a laser. Both were briefly described above. We return in

detail to the magnetic process. The reader who wants to know more about thermomagnetic writing can look up references [18] and [24].

4.1. FIELD PRODUCED BY A MAGNETIC HEAD

The theory of magnetic circuits immediately provides the field H_e inside the gap, with thickness g of a head excited by current I:

$$H_g = (nI/g)/(1+\ell/\mu g) \qquad (21.4)$$

Here n is the number of windings in the excitation coil and ℓ the average perimeter** of the magnetic circuit, μ its permeability. The factor $\eta = 1/(1+\ell/\mu g)$ is called the head efficiency. In the approximation $\mu g >> \ell$, we get:

$$H_g = nI/g \qquad (21.5)$$

but this formula of course does not describe the field to which the film is submitted.

In the simplified model of a head proposed by Karlqvist [25], the magnetic circuit is assumed to have infinite permeability, and to occupy the whole segment of space $0 < y < h_g$ ($h_g >> g$) in the orthogonal reference frame Oxyz (fig. 21.4). Oz is perpendicular to the plane of the figure and the circuit also includes a gap bounded by planes $x = -g/2$ and $+g/2$.

Relations (21.4) and (21.5) express the field *within* the gap. Karlqvist [25] assumes that the x component of the field H_x remains equal to H_g down to y = 0. Since the permeability of the magnetic circuit is taken as infinite, this implies that $H_x = 0$ for $x < -g/2$ or $x > +g/2$. Determining the field in the whole half-space $y<0$ then becomes a problem with specified boundary conditions for the tangential component of the field, hence for the magnetic potential, over the plane y = 0.

We know that the solution to this problem is unique, and it can be verified that a surface distribution of currents, with density $i_z = 2H_g$ on a band with width g, localised on the plane y = 0 between $x = -g/2$ and $x = +g/2$, creates at height $y = -\delta$, with δ positive but arbitrarily small, a field H_x precisely equal to H_g for $-g/2<x<+g/2$ and zero outside the same interval (fig. 21.4).

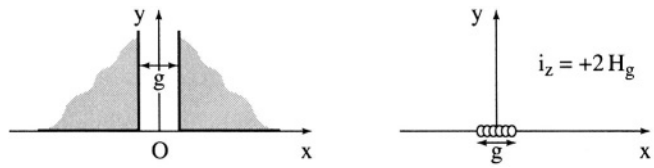

Figure 21.4 - Karlqvist's model

Left: schematic sketch of the region of the head gap near the recording media - Right: current distributions equivalent to the excited head for calculation of the field at y<0

** The average is weighted by the ratio of the cross-section of the gap to the local cross-sectional area.

The field created by this fictitious distribution in the whole half-space $y < 0$ is thus necesssarily the solution to our problem. It is obtained by summing the elementary contributions of infinite rectilinear currents $i_z\,dx' = 2H_g\,dx'$. The components obtained are $H_z = 0$ and:

$$H_x = -\frac{H_g}{\pi}\int_{-g/2}^{+g/2}\frac{1}{(x-x')^2+y^2}\,y\,dx'$$
$$H_y = \frac{H_g}{\pi}\int_{-g/2}^{+g/2}\frac{1}{(x-x')^2+y^2}\,(x-x')\,dx' \qquad (21.6)$$

After integration, this provides:

$$H_x = -\frac{H_g}{\pi}\left(\tan^{-1}\frac{x+g/2}{y} - \tan^{-1}\frac{x-g/2}{y}\right)$$
$$H_y = \frac{H_g}{2\pi}\ln\frac{(x+g/2)^2+y^2}{(x-g/2)^2+y^2} \qquad (21.7)$$

These functions are represented in figure 21.5 for various values of the ratio $|y|/g$.

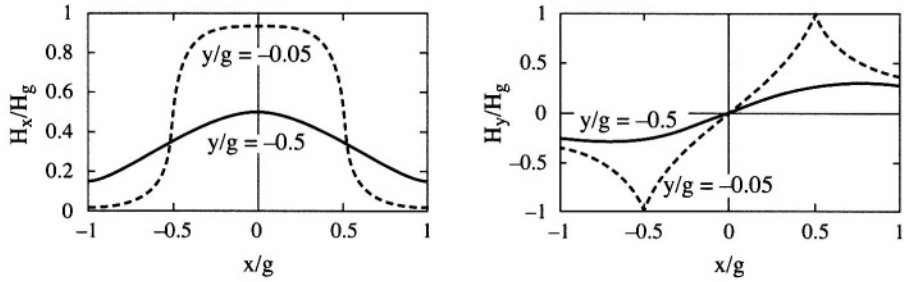

Figure 21.5 - Longitudinal (left) and vertical (right) fields at various distances from the head

In present-day equipments (in 1998), the correct approximation is $g >> \{h, y\}$, so that the profile of the field H_x is practically a *gate* function, equal to H_g between $-g/2$ and $+g/2$, and zero outside this interval. Near the edges of the gap, expression (21.7) can be simplified.

Thus, for x near $+g/2$, we have:

$$H_x \sim \frac{H_g}{\pi}\left(\frac{\pi}{2} - \tan^{-1}\frac{x-g/2}{y}\right) \qquad (21.8)$$

In what follows, we will rather use the field gradient:

$$\frac{dH_x}{dx} = -\frac{H_g/\pi\,y}{1+\left[(x-g/2)/y\right]^2} \qquad (21.9)$$

Karlqvist's model is rather satisfactory for the most classical heads, involving a ferrite circuit in which the length of the part in contact with, or very near, the medium is

indeed large with respect to the gap thickness, as in figure 21.4. This remains true in the most recent products, the *integrated planar* heads (fig. 21.6) [25].

In the so-called *vertical thin film* heads [14, 27], which appeared in the '80s, the magnetic circuit consists of soft magnetic films, which come near the medium in a plane perpendicular to the track, and whose thickness is not much larger than that of the gap (fig. 21.7). Karlqvist's model is clearly less adequate in this case. Calculations suited for this geometry were published as early as 1963 [28]. Numerical methods were also used (see for example ref. [26] for a well-documented review).

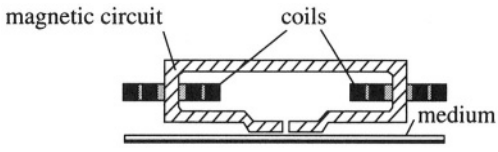

Figure 21.6
Principle of an integrated planar head

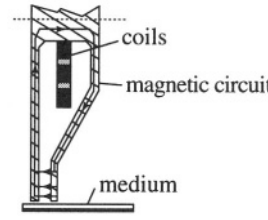

Figure 21.7
Principle of a "vertical thin film" head

Many models assume the permeability of the magnetic circuit to be infinite, or at least homogeneous and isotropic, and restrict the calculation to the static case. In more thorough models, where the ultimate limits are explored, in particular for thin film and integrated planar heads, sophistication is pushed far beyond the mere account of a finite homogeneous and isotropic permeability. This assumption is in fact not justified when the domain size is of the same order as the geometrical dimensions of the problem.The domain structure in the films must then be explicitly taken into account to determine (numerically) the response, which must furthermore be calculated in the dynamic regime. The reader can look up chapter 17 of the present book for more information on dynamic effects, and in particular the frequency dependence of response in a sinusoidal regime.

4.2. STABILITY OF WRITTEN MAGNETIZATION PATTERNS

The above section dealt with the shape of the field produced by the head, and we will later use these results to describe, at least in a semi-quantitative way, the write process. However, before tackling this problem, we investigate the conditions under which a *given* magnetization distribution in the film remains stable in the absence of a write field. This is one aspect of the basic problem of remanence stability, to be compared with the somewhat different view treated in section 3.1.2 of this chapter.

We define in a somewhat arbitrary way a standard distribution of magnetization, representative of those effectively encountered in written media:

$$M_x = M = (2/\pi)\, M_s \tan^{-1}(x/a) \qquad (21.10)$$

This *inverse tangent* distribution corresponds to an isolated transition from the saturated state with $M_x = -M_s$ to the saturated state with $M_x = +M_s$.

Here, Ox of course remains the axis parallel to the track, and we assume **M** to depend neither on coordinate z along the width of the track, nor on coordinate y along the medium thickness. We also neglect the perpendicular component M_y of **M**. The quantity 2a can be considered as the *length* of the transition.

This variation in magnetization produces a pole density $\rho = -\mathrm{div}(\mathbf{M}) = -dM/dx$ which is, in turn, responsible for a demagnetising field $\mathbf{H}_d$.

We can assume the thickness h of the magnetic film to remain very small with respect to the transition length 2a. This approximation is not mandatory, but it simplifies the calculations, it is consistent with the assumption on the uniformity of M(x) vs thickness, and it remains realistic enough.

The magnetic film then reduces to the plane Oxz carrying a *surface* distribution of magnetic masses, with density $-h(dM_x/dx)$. We then have:

$$2\pi(x - x')dH_d = -\left(\frac{2M_s h}{a\pi}\right)\left(\frac{dx'}{1 + (x'/a)^2}\right) \qquad (21.11)$$

Gauss's theorem is here used to express the elementary field produced at x by a line of magnetic masses, with linear density $-h(dM/dx')$, placed at x'. We note that this field has only one component, along Ox. We obtain:

$$H_d = -\frac{M_s h}{\pi^2 a}\int_{-\infty}^{+\infty}\frac{dx'}{(x - x')\left(1 + (x'/a)^2\right)} \qquad (21.12)$$

which, after some simple transformations, gives:

$$H_d = -\left(\frac{M_s h}{\pi a}\right)\left(\frac{x/a}{1 + (x/a)^2}\right) \qquad (21.13)$$

We see that the demagnetising field is zero at x = 0, i.e. at the middle of the transition. It is maximum, equal to $\pm(1/2)(M_s h/\pi a)$, for $x = \pm a$, respectively. If H_C is the coercive field of the material, the stability criterion is simply expressed as $(1/2)(M_s h/\pi a_0) = H_C$, hence:

$$2a_0 = M_s h/\pi H_C \qquad (21.14)$$

The *minimum* length of a *stable* transition is thus proportional to the spontaneous magnetization in the material, to the film thickness and to the reciprocal of its coercivity. Increasing the maximum density of bits (which is of the order of $1/2a_0$) thus requires either decreasing $M_s h$ or increasing H_C. However, as we will see later, it is not advisable to decrease $M_s h$, because this leads to a decrease in the read signal. This is why the improvements now considered for the materials bear mainly on the increase of the coercive field. We recall that formula (21.14) is based on the approximation $2a_0 >> h$, which implies $H_C << M_s/\pi$. If H_C becomes comparable to

M_s then a more exact calculation must be performed [14]. This leads, still under the assumption of a one-dimensional distribution of magnetization, to the conclusion that the transition can become infinitely steep provided $H_C \geq M_s$.

Another approach to evaluating the maximum density of stable bits in a medium starts from the assumption of a *sine-shaped* magnetization profile. The demagnetising field is again easy to calculate, as it was in the inverse tangent distribution we discussed above. The difference is that here we deal with the *magnetostatic* interaction *between bits,* and not just with the demagnetising effect of a single isolated transition. Let p be the period of the distribution (with p >>h), and $K = 2\pi/p$, so that:

$$M_x = M = M_s \sin(Kx) \tag{21.15}$$

We then find:

$$H_d = -(1/2)\,K\,M_s\,h \sin(Kx) = -(1/2)\,K\,h\,M \tag{21.16}$$

Applying the stability criterion $H_d = H_C$ leads to a minimum period p equal to:

$$p = 2\pi/K = M_s\,h/\pi H_C \tag{21.17}$$

This period should be compared to twice the length of the isolated transition, viz: $4a_0 = 2M_s\,h/\pi H_C$. We see that p is smaller by a factor two than $4a_0$, which practically means that a succession of transitions is more stable than a single isolated transition. This effect comes from the magnetostatic interaction between bits. A conservative value of the ultimate transition density will thus be: $1/2\,a_0 = \pi H_C/M_s\,h$.

4.3. WRITING A TRANSITION WITH A KARLQVIST HEAD

We just investigated the stability of a transition without asking how it was written. This allowed us in particular to determine the minimum length of this transition.

In a way, this length sets an ultimate limit, which depends only on the coercivity of the recording medium. However, we may also suspect the existence of another limit, possibly a more restrictive one, resulting from the write process itself. We now analyse this write process by considering that the medium remains fixed and that the head moves (fig. 21.8): let x be the coordinate linked to the track, u that linked to the head. The head, constantly fed with the nominal write current I, is moved from left to right on the track, which is initially magnetised in the negative direction. The write field is assumed to be positive, it thus tends to reverse the existing magnetization.

If the write current is large enough, we understand that moving the head produces a magnetization reversal front, *stationary with respect to the head,* near the leading edge of the gap. Behind the head, magnetization has flipped over by 180°.

In a first, very crude approximation, we can neglect the demagnetising field, hence assume that the material is only submitted to the *field from the head,* given by equation (2.1.8) with a change of x for u. Knowing the hysteresis loop of the material, we can then deduce the magnetization profile M(u) in the transition, at least if dynamic

effects are ignored (we assume that the material's response, as given by the hysteresis loop, is instantaneous).

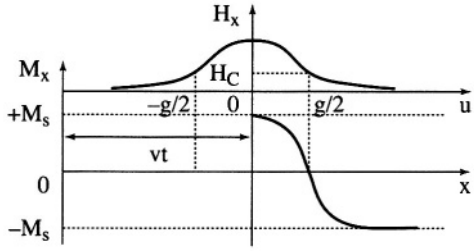

Figure 21.8 - Write process for a Karlqvist head

Actually, we are primarily interested not in a detailed knowledge of this profile, but only in obtaining a meaningful value for the length of the transition under the effect of the write field. We therefore just calculate the slope:

$$\frac{dM}{du} = \left(\frac{dM}{dH}\right)\left(\frac{dH}{du}\right) \approx \left(\frac{dM}{dH}\right)\left(\frac{H_g}{\pi y_0}\right)\left(\frac{1}{1+\left[(u-g/2)/y_0\right]^2}\right) \qquad (21.18)$$

where dM / dH is the slope of the rising branch of the hysteresis loop, and y_0 the distance between the head and the magnetic film, which is assumed to be thin with respect to y_0.

The parameter y_0 is commonly called the head spacing. We used the simplified expression (21.9) for the field gradient from the head. This gradient is a maximum for u = g/2, i.e. just below the leading edge of the gap. On the other hand, the slope of the loop dM/dH goes through a very sharp maximum, denoted by χ_{hy}, near the coercive field.

The maximum slope of the magnetization profile is thus obtained by setting the write current I so that H is equal to the coercive field precisely at the point where the field gradient of the head is a maximum. From (21.8), this implies $H_g = 2 H_C$, hence $H_g / \pi y_0 = (2/\pi) H_C / y_0$.

An approximate value of the transition length $2a_1$ is then obtained by writing $M_s / a_1 = dM / du$, which leads to:

$$2a_1 = \frac{2M_s y_0}{\chi_{hy} H_g} = \frac{\pi}{2} y_0 \frac{\Delta H}{H_C} \qquad (21.19)$$

where $\Delta H = 2 M_s / \chi_{hy}$ is a parameter which measures the *squareness defect* of the loop. The length of the transition under the write field is thus proportional to $\Delta H / H_C$ and to the head spacing y_0. However, we have till now not taken into account the demagnetising field H_d.

In Williams and Comstock's model [29], H_d is introduced in an approximate manner by *assuming* that the transition again has an inverse tangent profile as used above:

$$M = \frac{2}{\pi} M_s \tan^{-1} \frac{(u - g/2)}{a_2} \qquad (21.20)$$

Near the center of the transition, we have $M = (2/\pi) M_s (u - g/2)/a_2$. But, from equation (21.13):

$$H_d \approx -M_s h \frac{(u - g/2)}{\pi a_2^{\,2}} = -\frac{h}{2a_2} M \qquad (21.21)$$

This expression of the demagnetising field does not take into account the fact that the magnetic circuit of the head is nearby.

Equation (21.21) defines, near the middle of the transition, an *effective demagnetising field coefficient* $N = h/2a_2$. The material's response can then be expressed as a function of the head's field alone, provided the classical demagnetising field (shearing) correction +N M is applied to the *hysteresis loop* (see chap. 2 and 26). The main effect of this correction is that it increases the intrinsic squareness defect ΔH by an amount $2NM_s$, so that the transition length $2a_2$ becomes, using equation (21.19):

$$2a_2 = \frac{\pi}{2} y_0 \frac{\Delta H + 2NM_s}{H_C} = y_0 \left(\frac{\Delta H}{H_C} + \frac{M_s h}{H_C a_2} \right).$$

We thus obtain a self-consistency relation which takes the form of a second degree equation in a_2, with the physically satisfactory solution:

$$2a_2 = \frac{\pi}{4} y_0 \frac{\Delta H}{H_C} \left\{ 1 + \left[1 + \frac{16}{\pi} \frac{h}{y_0} \frac{M_s}{H_C} \left(\frac{H_C}{\Delta H} \right)^2 \right]^{1/2} \right\} \qquad (21.22)$$

This relation evidences the importance of the head spacing y_0, of the shape of the loop (through parameter $\Delta H/H_C$), and of the medium thickness h. However, a_2 does not vanish with ΔH, and it thus remains finite for a medium with a perfectly square loop. We note that the vicinity of the high permeability material of the head's magnetic circuit leads to a decrease in the demagnetising field of the transition. This effect can be taken into account in a rather simple way by altering the expression for the effective demagnetising field coefficient we introduced above. The result is a slight decrease in the length of the transition.

The transition length $2a_2$ is always larger than the ultimate minimum length $2a_0$, which confirms that the density limit of the write process is set by the head-medium interaction and not by the sole medium.

Williams and Comstock's analytic model –which we slightly simplified in this presentation– has the advantage of clearly indicating the influence of the various parameters, and of even providing quantitative predictions for the transition lengths which are quite sensible.

Nevertheless, the present tendency is to use numerical simulation. Then, using the actual shape of the medium's hysteresis loop, the head's field and the demagnetising field are rigorously calculated.

A simple method consists in starting from a first magnetising distribution, for example that resulting from Williams and Comstock's approximation. The field acting on the

material is then known, and from there a new distribution of magnetization is calculated via the hysteresis loop. Using successive iterations, the distribution is made to converge toward what is hoped to be the final and unique solution of the problem.

Values typical of the state of the art in 1997 are: $M_s = 1.1$ T; $\mu_0 H_C = 0.22$ T; $\Delta H / H_C = 0.2$; $h = 20$ nm; $y_0 = 20$ nm; $g = 0.2$ μm; ($g >> h, y_0$); such head spacings are actually obtained by quasi-direct contact through a solid lubrificant film (carbon) shared between the medium (typically 15 nm) and the head (typically 5 nm). The ultimate transition length as calculated from equation (21.14) is then $2a_0 = 0.03$ μm, and the write-limited transition length $2a_2$ turns out to be 0.08 μm from equation (21.22).

It can be assumed that two successively written transitions must be at least $2a_2$ apart to be correctly identified. In other words $2a_2$ is also the writing resolution. The above data show that, in the present heads, this resolution is notably smaller than the gap g. On the other hand, we will see that the reading resolution is always of the order of g, so that the limiting process in terms of usable information density is the read process.

5. THE READ PROCESS

The presence of a transition on the track can be detected by induction. In this case, a single head usually serves both for writing and reading, and the signal is, as we now show, proportional to $v dM/dx$ where v is the medium velocity. So-called magnetoresistive heads have recently appeared. Their response is also proportional to dM/dx but independent of v. We describe and discuss these two readout processes.

5.1. INDUCTIVE READOUT

An inhomogeneous distribution of longitudinal magnetization $M(x)$ necessarily entails a non-zero pole density and a demagnetising field, as discussed at length in the basic chapters of this book. The demagnetising field is not restricted to the magnetic film, it spills over into the neighbourhood. Detecting the transition is made possible by this *stray field.* In particular, the latter causes the induced flux variation in an *inductive head.*

To calculate this flux, we can use the very powerful *reciprocity theorem,* which was already used in chapter 17. A simple derivation is given in chapter 2.

Let $\mathbf{H}$ be the field produced at point P by the head when current I is passed through the coil. If the magnetic circuit of he head operates in the *linear* regime, $\mathbf{H}$ can be written in the form: $\mathbf{H} = \mathbf{C_H}\, I$, where the (vector) field coefficient $\mathbf{C_H}$ depends only on the point P considered. The reciprocity theorem then tells us that the flux Φ sent into the coil by a *point dipole* with magnetic moment $\mathbf{m}$ placed at P is given by $\Phi = \mu_0\, \mathbf{C_H}\, \mathbf{m}$. We are interested in the flux variation produced by the passage of a

transition under the head. This transition is characterised by a function **M** (x) of the coordinate x measured in a coordinate system moving with the track with velocity v. We assume again that **M** only has a longitudinal component:

$$M_x = M = (2M_s/\pi)\tan^{-1}(x/a_2).$$

The head's field coefficient profile is defined in the head's coordinate system, here assumed to be fixed, by a function $C_H(u)$, where C_H denotes the single longitudinal component of $\mathbf{C_H}$. The origin u = 0 is now chosen on the medium film, just below the middle of the gap. We decide that time zero corresponds to the two coordinate systems (u) and (x) having their origins in coincidence.

The element dx of the track, with width W, carries the moment m = M (x) W h dx. It induces in the readout coil the flux $d\Phi = \mu_0 C_H(u) M(x) W h\, dx$, where u = x + v t is the instantaneous abscissa of this element in the coordinate system linked to the head. The induced voltage is: $dV = -d^2\Phi/dt = -v h W \mu_0 M(x) dx\, G(x + v t)$, where $G(x + v t) = dC_H/du|_{u = x+vt}$. Thus we have:

$$V(t) = -v\mu_0 W h \int_{-\infty}^{+\infty} M(x)\, G(x + v t)\, dx \qquad (21.23)$$

To make calculations easier, we assume that the head spacing y_0 is much smaller than the width of the gap g, in agreement with the orders of magnitude given above. Then the function G(x, t) is approximately equal to:

$$G(x,t) = \frac{(C_H)_g}{\pi y_0}\left[\frac{1}{1+\left(\frac{x + vt + (g/2)}{y_0}\right)^2} - \frac{1}{1+\left(\frac{x + vt - (g/2)}{y_0}\right)^2}\right] \qquad (21.24)$$

Here $(C_H)_g$ is the head's field coefficient measured within the gap.

We can further simplify the calculation by assuming that a_2 is also much larger than y_0. Then the profile of G can be approximated by two Dirac peaks, each with content $\pi y_0 (C_H)_g / \pi y_0 = (C_H)_g$ centred respectively at – vt – g/2 and – vt + g/2.

The integral (21.23) reduces to:

$$V(t) = v W h \mu_0 (C_H)_g \frac{2}{\pi} M_s \left[\tan^{-1}\left(-\frac{vt}{a_2} - \frac{g}{2a_2}\right) - \tan^{-1}\left(-\frac{vt}{a_2} + \frac{g}{2a_2}\right)\right] \qquad (21.25)$$

It is worthwhile looking at two limiting cases. The first one is a bit academic, as it corresponds to $g << 2a_2$. The difference between the two inverse tangents is then practically a differential, and:

$$V(t) = \frac{1}{\pi} v W h \mu_0 (C_H)_g M_s \frac{g/a_2}{1 + (vt/a_2)^2} \qquad (21.26)$$

We thus have a *Lorentzian* voltage peak, with height proportional to $v W h (C_H)_g M_s g/a_2 = v W h \eta n M_s / a_2$ (remember that n is the number of windings and η the head's efficiency), with full width at half maximum, expressed in terms of the distance the tape has moved, equal to $2a_2$.

The other limiting case assumes that $g >> a_2$. The schematic behavior of V (t) is then close to a square pulse, with height proportional to $v\, W h \eta (n/g) M_s$, independent of a_2 and with width at half maximum equal to g.

In the general case where a_2 is of the same order of magnitude as g and where the head spacing and the medium thickness are no more neglected, it can be shown that the width at half maximum of the readout impulse corresponding to a transition (denoted as PW_{50} for *pulse width at 50%*) is given by:

$$PW_{50} = [g^2 + 4(y_0 + a_2)(y_0 + a_2 + h)]^{1/2} \qquad (21.27)$$

We note that this expression reduces to $[g^2 + 4a_2^2]^{1/2}$ if the head spacing y_0 and the medium thickness h are negligible with respect to g and $2a_2$. It is worth noticing that in the general formula, even if the transition is very steep $(a_2 = 0)$, the readout pulse retains a finite width, at least equal to the gap thickness. For 1997 heads, the orders of magnitude given above lead to $PW_{50} \sim 0.25\ \mu m$. We note that $PW_{50} > 2a_2$ (see § 4.3). In other words, as already noted in § 4.3, the maximum linear density of useful bits in the track is limited by the read process.

Another way of identifying the theoretical limits of the read process is to look at the response, *in terms of induced flux,* to a sine-shaped magnetization distribution. If $M(x) = M_s \sin(Kx)$, calculating $\Phi(t)$, in the approximation where y_0 and h are both very small compared to g and to the wavelength $\lambda = 2\pi/K$, yields:

$$\Phi(t) = -\frac{1}{2}\mu_0 W h g (C_H)_g M_s \sin(K v t) \frac{\sin(Kg/2)}{Kg/2} \qquad (21.28)$$

The readout flux is sine-shaped, with amplitude proportional to (2/Kg) sin (Kg/2). Therefore the *response involves zeros,* for characteristic wavelengths $\lambda_m = 2\pi/K_m = g/m$, with m an integer. This condition corresponds to the vanishing of the magnetic moment of the region of the film that is at any time submitted to the field of the gap.

In practice, a magnetic head is characterised [26] by using it first in the write mode, then in the read mode. First an AC square current, with variable amplitude and frequency, is fed into the head to write, at given speed, a periodic set of transitions on a *reference disk.* Then the voltage response to the recorded signal is recorded (fig. 21.9).

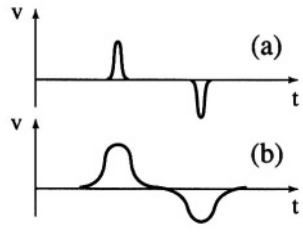

Figure 21.9 - Evolution of the shape of the read signal as a function of the written spatial frequency:
(a) low frequency
(b) high frequency

In the low frequency regime, the transitions are far from one another, and we measure voltage peaks with amplitude independent of the frequency, and width at half maxium equal, by definition, to that of an isolated transition (PW_{50}). With increasing frequency two phenomena occur. On the one hand, successive transitions start to overlap on writing, while the amplitude of the magnetization jump decreases. We thus approach a *sine-shaped* magnetization distribution, with *amplitude decreasing with f.* On the other hand, this effect superimposes on the read-mode response, as can be deduced from the transfer function given by equation (21.28).

For each value of the write current, the spectrum of the peak voltage vs spatial frequency, expressed as the number of flux reversals per mm of track length ($fr.mm^{-1} = flux$ *reversal per mm*), is plotted. Such a spectrum is shown in figure 21.10 after J.M. Fedeli [26] the maximum operating frequency is usually taken to correspond to a decrease by 50% in the head sensitivity with respect to its low frequency value.

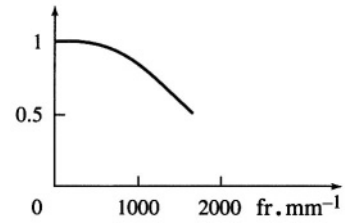

Figure 21.10 - Peak read voltage as a function of the written spatial frequency *(after [26])*

5.2. MAGNETORESISTIVE READOUT

The coupling between electric charge transport and magnetism is discussed in chapter 14, and *anisotropic magnetoresistance* in thin films, as well as *giant magnetoresistance,* which are of central interest here, are described in chapter 20.

Figure 21.11 shows the principle of a magnetoresistive sensor.

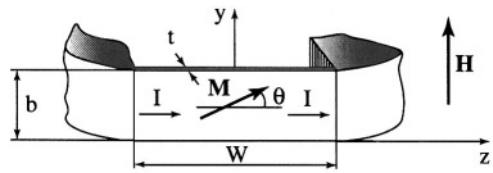

Figure 21.11 - Schematic description of the principle of a magnetoresistive sensor

The sensitive element is a soft magnetic thin film, typically a nickel iron alloy (Permalloy), with thickness t, width b (along Oy) and length W (along Oz). A current I is passed in the element (along the length W) and a voltage $V = \rho (W/bt) I$, proportional to the resistivity ρ of the alloy in the Oz direction of interest, is measured.

The film features a uniaxial anisotropy, with easy axis parallel to Oz (including in particular the shape contribution), and is characterised by the total anisotropy field H_A.

A first biasing field, small with respect to H_A, applied along Oz, is used to stabilise a single domain state. The field H to be measured is applied along Oy. It rotates the magnetization direction by an angle θ, leading to an induced component M_y. From chapter 20, we have $\sin\theta = H / H_A = M_y / M_0$ where M_0 is the spontaneous magnetization of the alloy. We also saw in chapter 20 that the *electrical resisitivity* of a ferromagnetic metal or alloy is different depending on whether it is measured parallel ($\rho_{//}$) or perpendicular ($\rho_\perp$) to magnetization. (The resistivity tensor has for its principal axes the magnetization direction and any two axes in the plane perpendicular to magnetization. Rigorously speaking, this is true only for amorphous or non-textured polycrystalline materials). Thus a uniaxial thin film will have resistivity ρ along the easy magnetization axis:

$$\rho = \rho_\perp + \Delta\rho \cos^2\theta = \rho_\perp + \Delta\rho\,(1 - H_y^2 / H_A^2)$$
$$= \rho_{//} - \Delta\rho\, H_y^2 / H_A^2 = \rho_{//} - \Delta\rho\, M_y^2 / M_0^2 \qquad (21.29)$$

where the parameter $\Delta\rho = \rho_{//} - \rho_\perp$ is positive and typically a few percent of $\rho_{//}$ or $\rho_\perp$. This law leads to a parabolic variation of the resistance R of a magnetoresistive element submitted to a uniform field H_y (fig. 21.12-a), up to a saturation field equal to H_A. In practice, the variation is parabolic only for fields much smaller than the anisotropy field H_A due to the non-uniformity of the transverse demagnetising field (fig. 21.12-b). As a result, there appears an inflection point, around which the response to small field variations is linear. A simple method for linearization thus consists in biasing the element to the inflection point through a second small DC field along Oy.

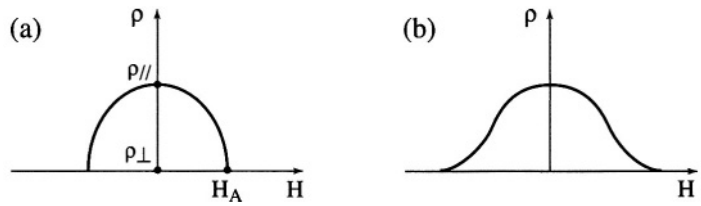

Figure 21.12 - Magnetoresistive effect in a thin film with uniaxial anisotropy
(a) theoretical behavior - (b) observed behavior

Another approach to linearization consists in passing the current at 45° to the easy magnetization direction, without biasing the film [30]. This technique is called "Barber pole" because it involves a pattern of highly conducting stripes (much better conductors than Permalloy!), which force the 45° direction for the current lines (fig. 21.13).

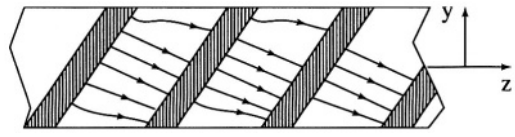

Figure 21.13 - "Barber pole" linearization technique

More information on biasing and linearization methods, and in particular those implemented in sensors for readout heads, is found in references [15, 31]. We now tackle the special application to readout heads. The field that must be detected is again the stray field of the recorded magnetic track. We place the magnetoresistive element as indicated in figure 21.14, the plane Oyz of the sensitive film being perpendicular to the axis Ox of the track.

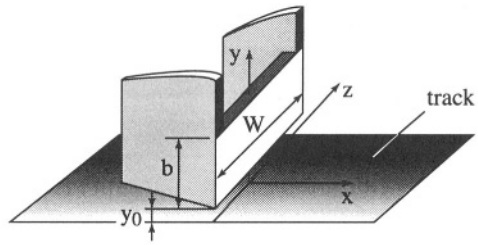

Figure 21.14 - Basic configuration of a magnetoresistive read head

When we discussed the inductive process, we saw that the stray field from the medium involves two components H_x and H_y. Component H_x is perpendicular to the sensitive field and produces only a very weak rotation of magnetization out of the Oyz plane. It can be neglected. We are thus interested only in measuring the field H_y parallel to the width b of the element. However, there appears an important difference with respect to the field sensor discussed above. Here H_y varies rapidly with the height y above the medium, and the element is therefore submitted to a highly inhomogeneous field.

Each elementary strip of the sensitive film, with width dy and length W, features a different variation in resistivity $D\rho(y)$. Due to the small values of the relative changes in resisitivity involved, it can be shown that the relative variation in resistance of the magnetoresistive element DR/R is given by:

$$\frac{DR}{R} = \frac{1}{b}\int_{y_0}^{y_0+b}\frac{D\rho(y)}{\rho}dy \qquad (21.30)$$

Here y_0 is again the head spacing, but the origin of the coordinates is taken on the magnetic track. We assume that the response of the magnetoresistive element is suitably linearised, so that we can write $D\rho(y)/\rho = \rho' M_y$. On the other hand, the sensitive film is also a *soft* magnetic layer ($H_A << M_s$). It therefore has high susceptibility, so that the *induction* B_y is practically $\mu_0 M_y$. Thus equation (21.30) can be written as:

$$\frac{DR}{R} = \frac{\rho'}{b\mu_0}\int_{y_0}^{y_0+b} B_y\, dy \qquad (21.31)$$

Imagine a coil, with axis Oy, involving n' windings per metre, with length b, is tightly wound around the magnetoresistive element. The flux Φ through the solenoid thus produced would be:

$$\Phi = n' t\, W \int_{y_0}^{y_0+b} B_y\, dy \qquad (21.32)$$

Thus the relative variation in resistance of the magnetoresistive element can be expressed in the form:

$$DR/R = \rho' \Phi / (b W t \mu_0 n') \tag{21.33}$$

Although it appears a bit artificial, this equation is valuable because it allows us once again to use the reciprocity theorem. Let $K_X(x, 0)$ be the x component of the field that would be created on the track if a current of 1 A were passed through the fictitious solenoid, with the soft yoke effect of the magnetoresistive film taken into account.

The flux induced in this fictive solenoid by the magnetization $M_x(x)$ of the written film (assumed to have small thickness h) is then:

$$\Phi = n' \mu_0 \int_{-\infty}^{+\infty} W h M(x) K_x(x,0)\, dx.$$

Whence:

$$DR/R = \rho' (h/bt) \int_{-\infty}^{+\infty} M(x) K_x(x)\, dx \tag{21.34}$$

This relation can be written in the equivalent form:

$$DR/R = \rho' (h/bt) \int_{-\infty}^{+\infty} \frac{dM_x}{dx} \Psi(x,0)\, dx \tag{21.35}$$

where $\Psi(x)$ is now the magnetic potential created by unit current density in the fictive solenoid. Note that here Ψ is, dimensionally speaking, a length.

In the simple configuration of figure 21.14, the field $K_x(x, 0)$ created by the fictive solenoid on the recording medium reduces, at least approximately, to that of two infinite lines of magnetic mass, with densities per unit length respectively $m' \sim -M_y t \sim -(M_0/H_A) n' t$ at $y = y_0$, and $+(M_0/H_A) n' t$ at $y = y_0 + b$, which leads to:

$$\Psi(x,0) = -\frac{M_0 t}{4\pi H_A} \ln\left(\frac{x^2 + {y_0}^2}{x^2 + (y_0 + b)^2} \right) \tag{21.36}$$

In this formula, we recall that M_0 and H_A characterise the magnetoresistive film, while in equation (21.34), $M(x)$ is the longitudinal magnetization of the track. The signal produced by the passage of an abrupt transition from $-M_s$ to $+M_s$ (which gives a Dirac peak with content $2M_s$ for dM_x/dx) is simply (with $b >> y_0$):

$$\frac{DR(x)}{R} \approx \frac{h}{b} \frac{\rho' M_0}{2\pi H_A} M_s \ln\left(\frac{x^2 + {y_0}^2}{x^2 + b^2} \right) \tag{21.37}$$

In this relation, x is the position of the transition. We check that the read signal, proportional to DR/R, is a peak centred on coordinate x = 0, with width at half maximum $2(b y_0)^{1/2}$. This width characterises the limitation in resolution due strictly to the magnetoresistive head. We note than the broadening due to the read process vanishes with the height, but, with the orders of magnitude for the state of the art in 1997 ($b = 0.6$ µm and $y_0 = 0.05$ µm), it turns out to be 0.35 µm. This value remains above that characterising the best inductive readout heads (see preceding section).

However the situation changes radically if *magnetic shields* are associated with the magnetoresistive element.

The implemented configuration is similar to that of vertical thin film inductive heads, at least very near the medium (fig. 21.15-a). The two soft shielding films are perpendicular to the track axis, and define a very thin gap where the magnetoresistive element is placed. The sizes indicated on the figure are given as an indication of the state of the art in 1997, and it must be kept in mind that evolution is very fast in this area.

The likeness to an inductive head disappears as soon as we move further from the recording medium. The shields have limited height, it is not necessary to close the magnetic circuit, and of course even less necessary to include a coil!

The response of such a head can again be calculated using the reciprocity theorem. The magnetic potential $\Psi(x, 0)$ produced on the recording medium by a fictive solenoid with the dimensions of the sensitive element and carrying unit current, is used.

In this approach, we can use the same assumption as Karlqvist, viz that the distribution of magnetic potential between the plates, which is linear in the center of the structure, is conserved as far as the end of the gap, i.e. to the plane $y = y_0$. The potential Ψ_t on this plane thus has the shape indicated in figure 21.15-b. It is a trapezoid with height $\overline{\Psi_t}$ and width at half maximum (1/2)(g + t) which can be decomposed into two Karlqvist potentials. Then the potential *at arbitrary height y* can be found analytically, using already established results (see § 4.1). The problem is thus reduced to determining $\overline{\Psi_t}$. This is done using the model of a line with distributed reluctance, similar to a tree-plate resistive line. More information can be found in the very detailed book by P. Ciureanu and H. Gavrila [15]. Here we just give some indications.

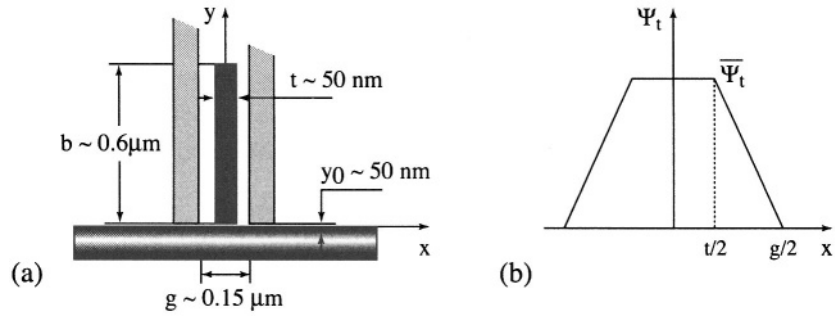

Figure 21.15 - Shielded magnetoresistive head

(a) geometry and axis definition

(b) shape of the magnetic potential induced by the fictive solenoid on plane $y = y_0$

In the distributed reluctance line model, the potential Ψ of the central plate (the sensitive film) and the flux Φ through it are functions of the single variable y, solutions to the differential equation system:

$$d\Phi/dy = -\Psi\Lambda' \; ; \; d\Psi/dy = n'I - \mathcal{R}'\Phi \qquad (21.38)$$

where $\mathcal{R}'$ is the reluctance per unit length of the central plane (the magnetoresistive film) and Λ' the permeance per unit length of the two half-gaps in parallel. n'I is the magnetomotive force per unit length associated with the fictive solenoid. It can be checked that $(\Lambda'\mathcal{R}')^{-1/2}$ is dimensionally a length, denoted as L_c.

If μ is the *intrinsic* permeability of the magnetoresistive film, then:

$$\mathcal{R}' = \frac{1}{\mu_0 \mu W t} \; ; \; \Lambda' = \frac{4\mu_0 W}{g - t} \; ; \; L_c = \frac{1}{2}[\mu t(g - t)]^{1/2} \qquad (21.39)$$

There exists a simple solution if the height b of the magnetoresistive element is small with respect to the characteristic length L_c. The variations of the potential and of the flux with y are then linear, and from symmetry we necessarily have $\Psi = 0$ at the centre of the element, i.e. at $y = b/2$. Then we can check that: $\overline{\Psi_t} = n'Ib/2 = n'b/2$ (since, from the very definition of Ψ, I = 1 A.

The potential on the exit plane of the gap is then a trapezoid with height n'b/2, with width at half maximum (g + t)/2, which can be used as the boundary condition for a combination of the two Karlqvist solutions, as we already explained. The result to be remembered is that, by adding shields, we recover readout pulses with width comparable to those of inductive heads.

But the significant advantage of magnetoresistive heads over their inductive counterparts is the *amplitude* of the output signal, and the fact that it is *independent of the head-track velocity.* Calculations show, and it is simple to check, that the readout signal corresponds practically to the saturation of magnetoresistance, in other words $DR/R \sim (\rho_{//} - \rho_\perp)/2\rho \sim 1\%$ to 2%.

The voltage picked up, $DV = I_0 DR = V_0 DR/R$ then depends only on the biasing voltage V_0 of the element. The latter is restricted by *thermal dissipation.* If P'_m is the maximum power that can be dissipated per unit area of the magnetoresistive film, then the optimum bias is: $V_0/W = (\rho P'_m)^{1/2} t^{-1/2}$.

An acceptable order of magnitude is $P'_m \sim 30\ \mu W.\mu m^{-2}$ (we note that this corresponds to $30\ MW.m^{-2}$!). As ρ is of the order of $20\ \mu\Omega.cm$ in the alloys used, we have: $(\rho P'_m)^{1/2} = (2.5\ V.m^{-1})^{1/2}$. With $t = 0.05\ \mu m = 5 \times 10^{-8}$ m and DR/R = 1%, we get $DV/W \sim 100\ \mu V.\mu m^{-1}$.

This value is roughly ten times higher than for an inductive head. For given amplitude, we can thus in particular *sharply decrease the track width* W. For given bit length, this is another way of increasing the density of information per unit area of a disk or tape.

These heads also have considerable potential for progress through a decrease in the thickness of classical materials, and the implementation of new materials featuring giant magnetoresistance effects (see chap. 20).

6. CONCLUDING REMARK

We did not mention, in this chapter, one aspect of disk or tape storage that deserves a lot of attention from the designer although it is not magnetic. This is the problem of the mechanical interaction between the medium and the head, which move at relative speeds ranging typically from 0.5 to $5\ m.s^{-1}$.

The present trend is to work practically at contact. This was always the case for tapes, but not for hard disk storage, where the head was made to literally fly at a fraction of a micrometer above the disk surface. The friction problems now become more serious than the aerodynamical problems. The interested reader can in particular look up reference [32].

REFERENCES

[1] S.H. CHARAP, PU-LING LU, YANJUN HE, Thermal stability of recorded information at high densities, *IEEE Trans. Magn.* **Mag-33** (1997) 978.

[2] D.A. THOMSON, J.S. BEST, The future of magnetic storage technology, *IBM Journal of Research and Development* **44** (2000) 311.

[3] Y. SONOBE, Y. IKEDA, Y. TAGASHIRA, Composite perpendicular recording media consisting of CoCrPt with large Hk and CoCr with positive inter particle interaction, *IEEE Trans. Magn.* **Mag-35** (1999) 2769.

[4] S.Y. CHOU, Patterned Magnetic Nanostructures and Quantised Magnetic Disks, *Proc. IEEE* **85** (1997) 652.

[5] Z.G. WANG, Y. NAKAMURA, Spin tunneling random access memory (STRAM), *IEEE Trans. Magn.* **32** (1996) 4022.

[6] M. JULLIERE, *Phys. Lett.* **54A** (1975) 225.

[7] J. ASHLEY, M.P. BERNAL, G.W. BURR, H. COUFAL, H. GUENTHER, J.A. HOFFFNAGLE, C.M. JEFFERSON, B. MARCUS, R.M. MCFARLANE, R.M. SHELBY, G.T. SINCERBOX, Holographic storage technology, *IBM Journal of Research and Development* **44** (2000) 341.

[8] P. VETTIGER, M. DESPONT, U. DRECHSLER, U. DüRIG, W. HÄBERLE, M.I. LUTWYCHE, H.E. ROTHUISEN, R. SCHUTZ, R. WIDMER, G.K. BINNIG, The "Millipede" - More than thousand tips for future AFM storage, *IBM Journal of Research and Development* **44** (2000) 323.

[9] J.C. MALLINSON, The foundation of magnetic recording (1987) Academic Press, New York-London.

[10] C.D. MEE, E.D. DANIEL, Magnetic recording (1990) McGraw-Hill, New York.

[11] J.J.M. RUIGROK, Short wavelength magnetic recording (1990) Elsevier, New York.

[12] H.N. BERTRAM, Theory of magnetic recording (1994) Cambridge Univ. Press.

[13] W.K. WESTMIJZE, *Philips Res. Rep.* **8** (1953) 148, article reproduit dans [2].

[14] R.M. WHITE, Introduction to magnetic recording (1986) IEEE Press, Piscataway, NJ.

[15] P. CIUREANU, H. GAVRILA, Magnetic heads for digital recording, *Studies in electrical engineering* **39** (1990), Elsevier, New York.

[16] S.B. LUITJENS, *in* High density digital recording, *NATO ASI Series E, Applied Sciences* **229** (1993) chap. 8, 217, K.H.J. Buschow, G. Long & F. Grandjean Eds, Kluwers Academic Publishers, Dordrecht.

[17] T. SUZUKI, *MRS Bulletin* **21** (1996) 42.

[18] M. MANSURIPUR, The physical principles of magneto-optical recording (1995) Cambridge Univ. Press.

[19] A.H. ESCHENFELDER, Magnetic bubble technology, *Springer Series in Solid State Sciences,* Vol. 14 (1980), Springer Verlag, Berlin-New York.

[20] D.F. EAGLE, J.C. MALLINSON, *J. Appl. Phys.* **38** (1967) 995.

[21] J.E. KNOWLES, *IEEE Trans. Magn.* **Mag-16** (1980) 62.

[22] J.L. DORMANN, D. FIORANI, E. TRONC, *Adv. Chem. Phys.* **98** (1997) 283.

[23] T.C. ARNOLDUSSEN, Film media, *in* Magnetic Recording Technology, 2nd ed. (1995) chap. 4, C.D. Mee & E.D. Daniel Eds, McGraw-Hill, New York.

[24] K.H.J. BUSCHOW, *in* High density digital recording, *NATO ASI Series E, Applied Sciences,* **229** (1993) chap. 12, 355, K.H.J. Buschow, G. Long & F. Grandjean Eds, Kluwers Academic Publishers, Dordrecht.

[25] O. KARLQVIST, *Trans. Royal Inst. Techn. Stockholm* **86** (1954), article reproduit dans [2].

[26] J.M. FEDELI, *in* High density digital recording, *NATO ASI Series E, Applied Sciences,* **229** (1993) chap. 9, 251, K.H.J. Buschow, G. Long & F. Grandjean Eds, Kluwers Academic Publishers, Dordrecht.

[27] R.E. JONES, W. NYSTROM, *U.S. Patent* 4 190 872 du 26 février 1980.

[28] I. ELABD, *IEEE Trans. Audio* **Au-11** (1963) 21.

[29] M. WILLIAMS, R. COMSTOCK, *AIP Conf. Proc.* **1**, No 5 (1971) 738, article reproduit dans [2].

[30] K.E. KUIJK, W.J. VAN GESTEL, F.W. GORTER, *IEEE Trans. Magn.* **Mag-11** (1975) 1215.

[31] J.C. MALLINSON, Magnetoresistive heads. Fundamentals and Applications (1996) Academic Press, New York-London.

[32] BHARAT BHUSHAN, *in* High density digital recording, *NATO ASI Series E, Applied Sciences,* **229** (1993) chap. 10, 281, K.H.J. Buschow, G. Long & F. Grandjean Eds, Kluwers Academic Publishers, Dordrecht.

[33] C.D. MEE, E.D. DANIEL, Magnetic recording (1987) McGraw-Hill, New York.

[34] A.S. HOAGLAND, J.E. MONSON, Digital magnetic recording, 2nd ed. (1991) John Wiley & Sons, New York.

[35] J.J.M. RUIGROK, Short wavelength magnetic recording (1990) Elsevier, New York.

[36] J.C. MALLINSON, The foundation of magnetic recording (1987) Academic Press, New York-London.